Journal of Scientific & Industrial Research
Vol. 83, July 2024, pp. 730-740
DOI: 10.56042/jsir.v83i7.10082

Impact of RoPP in Wavelength Conversion Inducing Nonlinearity and All-Optical 3R Regeneration for DWDM Networks

Parashuram[1,2] & Chakresh Kumar[1]*

[1]University School of Information, Communication and Technology, Guru Gobind Singh Indraprastha University, New Delhi 110 078, India

[2]Department of Electronics and Communications Engineering, Bharati Vidyapeeth's College of Engineering, Delhi 110 063, India

Received 02 April 2024; revised 13 May 2024; accepted 23 May 2024

The effect of Rotation of Plane of Polarization (RoPP) on wavelength conversion-induced nonlinearity and all-optical 3R regeneration has attracted significant attention in the quickly changing field of Dense Wavelength Division Multiplexing (DWDM) networks, where high-capacity data transmission is critical. This paper explores the complex interactions among RoPP, wavelength conversion, and 3R regeneration, focusing in particular on modeling and assessing the Bit-Error-Rate (BER) and Quality-factor (Q) variations under different polarization rotational angles. In nonlinear media, the 1545 nm Gaussian probe signal interacts with the 1554 nm CW (Continuous Wave) pump signal to cause Cross-Phase Modulation (XPM), which is used to convert wavelengths using nonlinear polarization rotation. Our study presents a theoretical framework that includes RoPP modulation, Variable Optical Attenuators (VOAs), Highly Nonlinear Fiber (HNLF), Clock, and Travelling Wave SOA (TWSOA) as major components to support the possibility of using polarization manipulation to reduce nonlinear impairments and improve network performance as a whole. Using TWSOA integrated 3R regeneration, the results show that the highest/lowest realized quality factor is 28.89/24.54 and the lowest/highest value of Log of (BER) is −179.35/−132.64. It finds out that 3R regeneration improves quality factor by more than 19 at a 90-degree rotational angle, and as a result, BER is significantly decreased. Findings confirm symmetry on both sides with reference to orthogonal polarization. The results of this study open new directions for the development of novel approaches to strategically manipulate the polarization state of light in order to optimize DWDM network performance and overcome the problems of nonlinearities and signal degradation in high-capacity optical communication systems.

Keywords: 3R Regeneration, Cross-phase modulation, Nonlinear fiber, Plane of polarization, Wavelength conversion

Introduction

In order to meet the growing need for high-capacity data transfer, Dense Wavelength Division Multiplexing (DWDM) technology has developed to the point where several wavelengths can be sent over a single optical fiber. However, signal deterioration and nonlinear constraints prevent DWDM networks from reaching their full potential. This paper investigates new ways to address these issues, with particular attention to wavelength conversion and all-optical 3R regeneration, where the RoPP is adjusted. The modulation of the polarization state of light, in particular RoPP, affects the signal quality and nonlinear effects. Our goal is to present a thorough knowledge of the connection between the possibility of all-optical 3R regeneration, wavelength conversion-induced nonlinearity, and RoPP modulation. Recently, various new methodologies are used to demonstrate the evolution of optical fiber communication in relation to regeneration, wavelength conversion, and polarization modulation is demonstrated.[1–3] In optical networks, the wavelength conversion using the nonlinearity is critical in terms of polarization condition of light. Advanced modulation formats, such as Gbps PolSK-DP-DQPSK orthogonal modulation, can significantly improve the spectral efficiency of long-haul DWDM optical systems.[4–6] To achieve longer transmission lengths, dispersion correcting methods including EDFA were applied. The suggested orthogonal modulation requires a high SNR, which is met via EDFA amplification. The future prospects of polarization-independent wavelength conversion and all-optical regeneration incorporating advance modulation and an orthogonal pump for polarization multiplexing is investigated. To improve network efficiency and reduce blocking probabilities, AOWC is required to eliminate wavelength conflict during dynamic optical path switching at nodes.[7–8]

*Author for Correspondence
E-mail: chakreshk@ipu.ac.in

Wavelength conversion at important network nodes enables the introduction of multiplexing ideas such as DWDM for more efficient bandwidth utilization.

Wavelength conversion at important network nodes enables the introduction of multiplexing ideas such as DWDM for more efficient bandwidth utilization. Cross Polarization Modulation (XPolM) is useful in wideband Semiconductor Optical Amplifiers (SOAs) to accomplish AOWC because SOAs have the essential nonlinearity. The efficiency of AOWC for the CSRZ-DPSK data format is evaluated using the input pump power dependent polarization rotation.[9] In order to realize polarization independent wavelength conversion using advanced modulation techniques like PDM-16QAM and PDM-(DP)QPSK, PDM and PDL are crucial challenges. A significant solution to such polarization-related problems is the vector distribution of PMD and addition of nonlinearity using parallely coupled dual TWSOA in conjunction with co-polarized dual pumps.[10–12] For accurate state of polarization optimization, signal quality is not assessed for different rotational angles in any of these proposed investigations. PMD and PDL losses caused by different nonlinearities over the fiber link are investigated.[13] The numerous methods of wavelength conversion and 2R regeneration in SOA, polarization modulation, and the generation of nonlinearities making use of SOA in recent times is presented recently.[14–16] Although all of these techniques are efficient and have many benefits, they also have certain disadvantages, including a decrease in signal quality because of polarization dispersion losses, a lack of optimization in relation to the polarization rotator angle, and an inefficient trade-off between data rate, power, and polarization angle. With the advent of the multiple-channel wavelength multicasting technique, which uses a single silicon waveguide for effective signal routing and high-speed data transmission, optical communication technology has advanced. The use of Four-Wave Mixing (FWM) procedures in conjunction with angled-polarization pumps in a single silicon waveguide to demonstrate five multicast channels customized for the two polarization channels of the fast 40 Gbit/s PDM-QPSK signals is realized recently.[17] Nevertheless, for best results, issues like nonlinear effects and pump power requirements is be resolved. It is established that an optical regenerative wavelength conversion technique can increase the dispersed satellite network's wavelength usage ratio.[18] Because the time it takes for a carrier to recover is smaller than the pulse width, this system uses Self-Phase Modulation (SPM) and FWM in SOAs to extend the signal spectrum toward both higher and lower frequency. A potential all-optical 2R (re-amplification and re-shaping) regenerator-based wavelength conversion method makes use of nonlinearity.[19] In order to retrieve the frequencies produced by chirping, the regenerator converts continuous wave to pulsed wavelength via offset filtering. Better resilience to amplified spontaneous emission noise is achieved by including the regenerator, according to performance evaluations conducted at various optical signal to noise ratios using BER analyzer. The Manakov equation is used to study the nonlinear propagation features of the Polarization-Division-Multiplexing (PDM) signal, which describes the nonlinear interaction of orthogonally polarized photons.[20] To achieve high-quality transmission via an optical link in such methods, Polarization-Dependent Loss (PDL) is a significant obstacle. Through numerical computation, it is discovered that when processing nonorthogonal PDM signals, the nonlinear wave equation assuming orthogonal PDM signals leads to insignificant inaccuracies in effect. It has recently been shown that dispersive bistability and two nonlinear polarization rotations can occur simultaneously.[21] A measured orthogonality of 30% is correlated with bistable hysteresis in the Stokes parameters. A nonlinear polarization rotation-based short wavelength harmonically mode-locked thulium-doped fiber laser is developed.[22] A record short wavelength of 1787 nm and FWHM of 6.5 nm are attained for stable soliton pulsing. Signal quality deteriorates as a result of significant imperfections like polarization mode dispersion (PMD) and PDL caused by the polarization difference between adjacent channels. In a high bit rate optical link, PMD sets a restriction on the transmission speed and distance. PDL causes signal distortions and a rise in bit error rate by altering the polarization of light in neighboring channels such that it travels in the optical fiber at slightly different speeds. Optical phase conjugation effectively reduces impairments by precisely reversing the amplitude and optical phase distortions that a signal undergoes. Through dispersion adjustment modules, OPC reduces the impact of chromatic dispersion.[23] The potential use of SOAs as an integrable broadband amplifier in commercial transponders and as a nonlinear medium for optical signal processing—particularly for optical channels with sophisticated modulation formats—are made possible by advancements in fabrication technology and device design. With a focus on all-optical wavelength conversion, optical phase conjugation, and phase quantization of coherent optical signals, SOAs play a part in optical signal processing techniques as well as low-distortion amplification of phase-modulated signals.[24] All-optical wavelength conversion and signal regeneration with a focus on reshaping are demonstrated.[25] The extinction ratio, PMD, and signal pulse width are used to evaluate the converted signal's quality. It is demonstrated that sigmoid transfer function can be performed by an optoelectronic artificial neuron model. The suggested optoelectronic circuit based on nonlinear polarization rotation (NPR) may mimic the functions of a continuous sigmoidal neuron with only one SOA.[26] Bias current, probe beam strength, and initial State Of Polarization (SOP) all influence the proposed neuron's response to excitatory and inhibitory inputs. By altering the initial SOP, the neuron's likelihood of being stimulated or inhibited can be changed. It is reported on an optical method that uses nonlinear polarization rotation in extremely nonlinear fiber to generate Frequency-Shift Keying (FSK) RF signals.[27] With a 10 GHz carrier, FSK RF signals are produced at 1.25 and 2.5 Gbps. Bulk SOAs co-integrated with AWGs are used to demonstrate a Polarization-Insensitive Photonic (PIC) integrated 1×4 WDM wavelength selective switch.[28] It is found that up to 25 Gbps NRZ-OOK, net gain, broadband, and error-free operation may be achieved with a 0.6 dB power penalty. For a 200-Gbps wavelength conversion, a delayed-interference all-optical semiconductor gate assisted by nonlinear polarization rotation has been studied.[29] The NPR in the SOA greatly affects the high-frequency operation of a Delayed-Interference Signal-Wavelength Converter (DISC) using a cross-correlation system with a temporal resolution of 1.5 ps, which was developed to monitor our 200-Gbps, 4992-bit-long binary-patterned waveforms. The Pattern-Induced Intensity Fluctuation (PIF) was greatly enhanced when the NPR effect inside our DISC was experimentally tuned. With the new gate model, the qualitative explanation of the PIF's dependence on the polarization settings was provided. An investigation is conducted into a Cross Phase Modulation (XPM) on SOA based wavelength conversion.[30] At the SOA's output, nonlinear rotation in the polarization state causes the wavelength conversion. Optimizing the different SOA settings improves nonlinear polarization rotation. Up and down conversion with non-return to zero input signals at a data rate of 10 Gbps is accomplished with a wavelength separation of 1 nm.

Optoelectronic oscillators are used to illustrate clock recovery for OTDM at 40 Gbps, 100 Gbps, and 160Gbps.[31] For 3R regenerations at 40 Gbps and 100 Gbps, Fabry-Perot cavities with SOA post processing are used. Using a counter propagation setup and a very low power pumping approach, cross polarization modulation in SOA based wavelength conversion is demonstrated. A minimum pump power of −4 dBm is used to replicate this strategy at a data rate of 80 Gbps.[32] Subsequently, the impact of pump power and the dynamics of the polarization state are characterized in order to assess the feasibility of converting all optical wavelengths. As a result, a minimal logarithmic bit error rate of −33.8 and an acceptable quality factor of 12.73 are obtained for an error-free wavelength conversion. An all optical up and down wavelength converter based on the XPolM effect in semiconductor optical amplifier Mach-Zehnder Interferometer (SOA-MZI) is tested and evaluated for error free operation in order to demonstrate the viability of a 40 Gbps differential phase shift keying modulated data signal.[33] The wavelength conversion is achieved through the revolving state of polarization of the pump and probe signals in SOA. The impact of variable signal power in combination with different SOA parameters on the performance of converted wavelength signal in terms of optical reception power and Q-factor has been investigated in order to enhance the scalability and accessibility of future hybrid optical access networks.

In summary, this review of the literature identifies a number of gaps in our current understanding, including the fact that the quality factor and BER of the obtained signal are uncorrelated with the polarization rotator angle, that 3R regeneration is not well optimized, and that signal quality deteriorates at data rates higher than 200 Gbps. Additionally, it creates the foundation for a thorough analysis of the effect of RoPP on wavelength conversion and 3R regeneration for the purpose of optimizing DWDM network performance.

Theoretical Framework

The term 3R refers to the three primary functions of this regeneration process: re-amplification, re-shaping, and re-timing. The weakened optical signal is amplified to restore its original power level, ensuring that it is strong enough for the following stages of the communication link. During transmission, the amplified signal may experience distortions such as waveform degradation or jitter. Re-shaping the signal entails restoring its original shape, minimizing signal distortions, and preparing it for further propagation. Signal propagation time variations can cause timing misalignments. By adjusting the signal timing, aligning it with the reference clock, and optimizing the temporal characteristics of the signal, re-timing ensures synchronization.

To simulate the effect of RoPP on wavelength conversion with and without 3R regeneration, we can consider variations in the XPM-induced phase shift, converted wavelength, Quality-factor (Q), and BER as functions of rotational angle (θ). Phase shift caused ($\Delta\emptyset_{RoPP}$) caused by XPM with RoPP is given by Eq. (1)

$$\Delta\emptyset_{RoPP} = -\gamma P_{m,pump} L A(\theta) \quad \text{... (1)}$$

where, $P_{m,pump}$ is the peak power of the pump signal, γ is nonlinear coefficient, L is the length of nonlinear medium HNLF, and RoPP coefficient is denoted as $A(\theta)$. The signal wavelength after XPM induced conversion with RoPP is expressed as Eq. (2)

$$\lambda_{RoPP} = \lambda_{signal} + \Delta\lambda_{RoPP} \quad \text{... (2)}$$

where, λ_{RoPP} is converted wavelength, λ_{signal} is original signal wavelength, and $\Delta\lambda_{RoPP}$ is the change in wavelength due to RoPP employed pump-probe combination of XPM. The Q-factor is typically described as the ratio of peak amplitude of the signal waveform to the root mean square (RMS) value of the noise.

The variation in Q factor caused by RoPP is defined as follows in Eq. (3)

$$\Delta Q_{RoPP} = -\frac{\Delta\emptyset_{RoPP}}{\pi} \quad \text{... (3)}$$

The Q factor of the converted signal (Q_{RoPP}) can then be calculated by adding ΔQ_{RoPP} to the original signal Q factor (Q_{signal}) as Eq. (4)

$$Q_{RoPP} = Q_{signal} + \Delta Q_{RoPP} \quad \text{... (4)}$$

The variation in BER is caused by XPM induced wavelength conversion can be expressed as follows in Eq. (5)

$$Q_{RoPP} = Q_{signal} - \frac{\Delta\emptyset_{RoPP}}{\pi} \quad \text{... (5)}$$

The effect of RoPP on BER is given by Eq. (6)

$$\Delta BER_{RoPP} = \frac{1}{2} erfc\left(\frac{\Delta Q_{RoPP}}{\sqrt{2}}\right) \quad \text{... (6)}$$

where, erfc is the complementary error function. The polarization angle (θ) is related to the RoPP coefficient $A(\theta)$ and its variation with respect to θ can be modeled as Eq. (7)

$$A(\theta) = A_p \cos^2(\theta - \theta_p) \quad \text{... (7)}$$

where, A_p is the peak RoPP coefficient and θ_p is the reference polarization angle. According to this equation the RoPP effect is maximized when the polarization angle coincides with the reference angle θ_p. Taking into account the effects of BER and polarization angle after RoPP, the Q factor and BER after 3R regeneration are expressed as follows in Eq. (8) & (9)

$$Q_{3R} = Q_{RoPP} + f(BER_{RoPP}, \theta) \quad \text{... (8)}$$

$$BER_{3R} = BER_{RoPP} g(\theta) \quad \text{... (9)}$$

where, $f(BER_{RoPP}, \theta)$ is a function that represents the impact of bit error rate and rotation angle with 3R regeneration. The function accounts for differences in signal quality with different polarization angles, taking into account the optimal polarization angle for minimum distortion. The function includes terms indicating the effectiveness of 3R regeneration in mitigating signal distortions and lowering BER. The presence of mechanism for re-amplification, reshaping, and retiming of the optical signal implies the presence of 3R regeneration. $g(\theta)$ is a function that captures the impact of the polarization angle on BER after 3R regeneration. These equations provide a conceptual framework for simulating RoPP's effect on wavelength conversion with and without 3R regeneration. The specific form of the function $f(BER_{RoPP}, \theta)$ would be determined by system characteristics and experimental observations as in Eq. (10)

$$f(BER_{RoPP}, \theta) = k_1 BER_{RoPP} + k_2(\theta - \theta_p)^2 + k_3 BER_{RoPP}(\theta - \theta_p) \quad \text{... (10)}$$

k_1, k_2, and k_3 are coefficients that represent the effect of BER and polarization angle on the regeneration process. θ_p denotes the reference polarization angle. The linear term ($k_1 BER_{RoPP}$) represents the linear effect of BER on the regeneration process. The regeneration process may become more difficult as BER rises. The quadratic term ($k_2(\theta - \theta_p)^2$) expresses the regeneration process's quadratic dependence on rotational angle. It takes into account non-linear effects caused by the polarization angle. The interaction between BER and rotational angle is represented by the cross-term ($k_3 BER_{RoPP}(\theta - \theta_p)$). This term enables the function to take into account potential synergies or interferences between these two factors.

System Overview and Operation

The proposed simulation configuration to understand the impact of RoPP in XPM induced wavelength conversion and all optical 3R regeneration, is depicted in Fig. 1. Input wavelength channel, optical amplifiers, Nonlinear XPM medium for wavelength conversion units, polarization transformer, clock, as well as power supplies and 3R regeneration unit, are all included in the proposed system schematic. Each component contributes to the overall functionality of the system. A 300 Gbps data stream with a defined pattern is produced by the PRBS (Pseudo-Random Bit Sequence) Generator and fed into the optical communication system.

The PRBS acts as a regulated source of input signals with predetermined bit sequences for XPM-based wavelength conversion testing and analysis. The wavelength of 1545 nm is defined by the optical pulse generator at 10 dBm launch power, which transforms the electrical signal into optical pulses from the electrical signal coming from the PRBS generator, ensures that the input for the XPM process is in the optical domain by starting the optical signal.The optical signal's polarization state is rotated using a polarization rotator in order to examine the effects of various rotational angles (θ) on wavelength conversion generated by XPM. The optical signal is amplified by an EDFA (Erbium-Doped Fiber Amplifier) to make up for propagation loss, ensures a robust contact by increasing the signal power prior to it entering the HNLF for efficient XPM. As illustrated in Fig. 1, the optical spectrum analyzer at the output of EDFA 1 displays the optical power as a function of wavelength. The optical power meter at the output of EDFA 1 indicates that the received optical power is 9.99 dBm. To improve the effectiveness of the XPM process, optical bandpass filters are employed to isolate the targeted wavelengths and ensure that only the required wavelength range reaches the HNLF. The probe wavelength, 1545 nm, is isolated using optical filter 1 to exclude undesired sidebands. Variable Optical Attenuator 1 (VOA 1) modifies the power of the optical signal. The pump and signal are combined into a single waveguide via an optical coupler. Continuous Wave Pump (CW Pump) delivers an optical pump signal of 1554 nm at 10 dBm launch power. The pump and signal are combined into a single waveguide via an optical coupler. Optical Coupler 1 permits effective XPM interaction, enabling the pump to adjust the signal by utilizing the HNLF medium's nonlinear characteristics. Strong nonlinearity and XPM are caused by HNLF (Highly Nonlinear Fiber) due to its nonlinear optical characteristics. facilitates the interaction between the modulated signal (1545 nm) and the continuous-wave

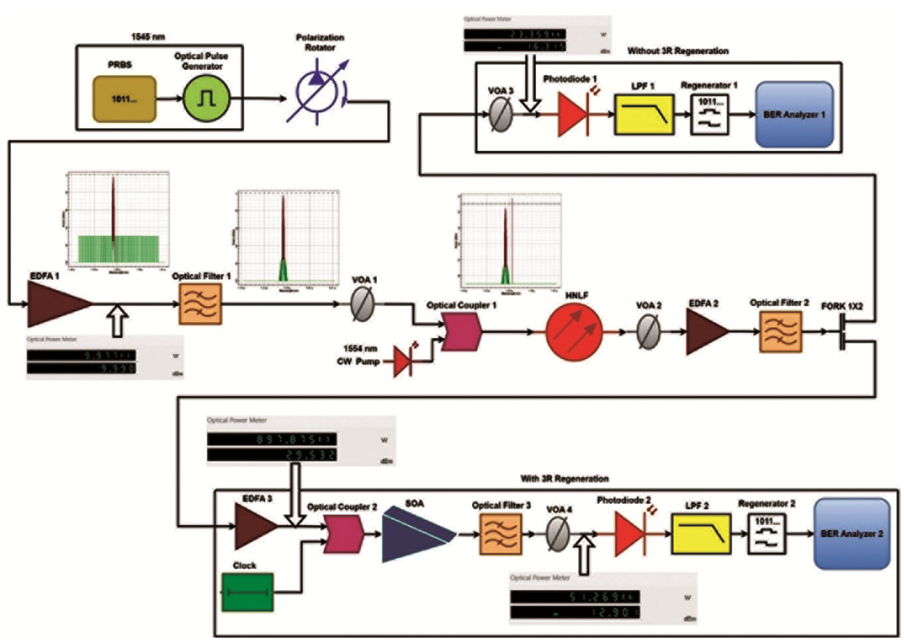

Fig. 1 — Simulation setups to realize the impact of RoPP in wavelength conversion using XPM medium and all optical 3R regeneration

pump (1554 nm) during wavelength conversion. Phase shift experiments caused by XPM are made possible by controlled variations in the optical signal power, which is regulated by the variable optical attenuator 2 (VOA 2). The XPM induced signal is amplified by EDFA 2. Optical filter 2 is used to isolate the targeted (converted) wavelength 1554 nm. Additionally, Fork 1 × 2 splits the signal into two routes so that it can be independently analyzed with and without 3R regeneration 3 and VOA 4 are used, respectively, to adjust the amplitude of the wavelength-converted signal with and without 3R regeneration. At the output of VOA 3 and VOA 4, the received power is −16.315 dBm and −12.901 dBm, respectively. The recovery of the original data from the optical signal is aided by coupling a clock with an optical signal acquired from EDFA 3 using Optical Coupler 2, and the optical power meter at EDFA 3 indicates that the power received there is 29.532 dBm. Timing inconsistencies and data errors are avoided by using the clock signal to guarantee that data processing and transmission happen at the appropriate times. TWSOA enhances signal quality, facilitates clock extraction and ensures appropriate signal shape. To detect the transformed signal and convert it back to an electrical signal, photodiodes are utilized. High-frequency components that were added during XPM but are no longer required are eliminated by the Low Pass Filters (LPF 1 and LPF 2). The best wavelength conversion conditions at various rotational angles are determined by measuring the impact on signal quality, which is done by the BER analyzer. The method looks into how polarization affects wavelength conversion produced by XPM by varying the polarization rotational angle (θ). With an emphasis on the effects of different rotational orientations, this proposed diagram highlights the components and their roles in a wavelength conversion system based on Probe Pump-Induced XPM both with and without 3R regeneration.

Results and Discussion

The proposed configuration depicted in Fig. 1 is used to run the simulations. For simulation, we took into account a sampling rate of 1920×10^9 samples per second samples and a resolution of 0.1 nm. Through a polarization transformer, a 300 Gbps Gaussian optical probe signal of 1545 nm wavelength with 10 MHz line width is transmitted for rotations ranging from 0 to 180 degrees. Both Optical Filter 1 and Optical Filter 2 have a 400 GHz bandwidth and are Gaussian optical filters. The central frequency of Filter 1 is 1545 nm, whereas Filter 2 has an adjustable central frequency. A CW laser transmits a pump signal with a frequency of 1554 nm (targeted wavelength) and a noise figure of 3 dB. The HNLF's simulation parameters are as follows: dispersion of −0.1ps/nm/Km, dispersion slope of 0.0074 ps/nm^2/Km, attenuation inside the fiber is 0.2 dB/Km and effective area of 12 μm^2. The cutoff frequency of the Low Pass Gaussian filters (LPF 1 and LPF 2) is 60 GHz. The photo detector PIN simulation parameters are as follows: load resistance of 50 Ω, responsivity of 1 A/w, junction capacitance of 3 pf, and dark current of 10 nA. Furthermore, TWSOA has a carrier density of $1.42 \times 10^{24}\ m^3$ and an optical confinement factor of 0.3.

The optical spectrum analyzer (OSA) plot at the HNLF output is displayed in Fig. 2(a). It displays the received power at HNLF as a function of various wavelengths. As can be seen in Fig. 1, the OSA at the EDFA1 indicates that the noise level is −70 dBm and the received power of the 1545 nm probe signal is −2 dBm. Prior to wavelength conversion, noise power was lowered to −75 dBm by using filter 1. Following the coupling of the 1545 nm probe signal and the 1554 nm pump signal using Optical Coupler 1, the probe signal's received power is −4 dBm, the noise power is −75 dBm, and the pump signal's received power is 7 dBm at 1554 nm. Cross Phase Modulation happens because of probe-pump interaction over nonlinear medium. As illustrated in Fig. 2(a), the nonlinearity introduced by HNLF causes the received power of the 1545 nm probe signal to drop to −8 dBm and the received power of the 1554 nm pump signal to drop to 5 dBm. Phase shift on the probe signal, aided by the pump signal and generated by the XPM interaction across the HNLF medium, is demonstrated by OSA. With the same information as the initial probe signal, this phase shift causes a wavelength shift from 1545 nm to 1554 nm. Peaks at certain extra frequencies that correspond to Brillouin or Raman shifts can be seen in the OSA graphic. The received power as a function of wavelength/frequency is displayed on the OSA plot. The extremely nonlinear fiber generates a variety of additional distorted spectral patterns, or sidebands, through a process called supercontinuum production. The additional nonlinearity has widened the spectrum, but two prominent peaks at 1545 and 1554 nm show that the

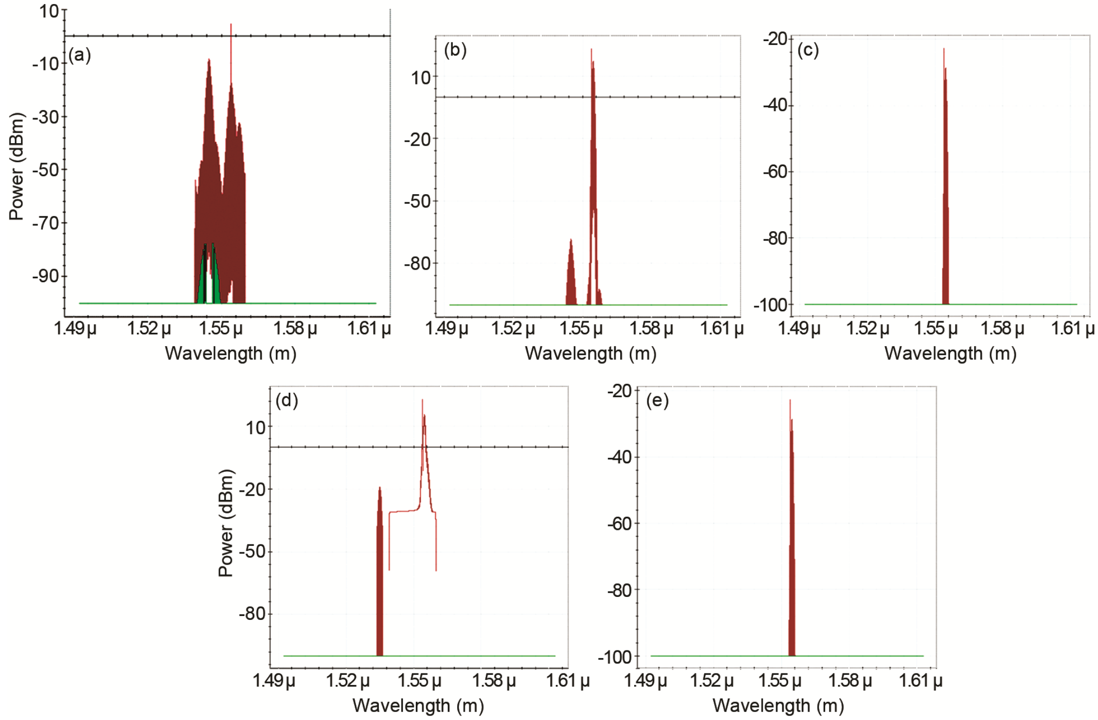

Fig. 2 — (a) The post-conversion optical spectra at the HNLF following the interaction of the pump signal (1554 nm) and probe signal (1545 nm) over the XPM medium, (b) The post-conversion optical spectra at the EDFA 3 in 3R regeneration path, (c) Optical spectra at the output of VOA 3 via 'without 3 R regeneration path', (d) Optical spectra at the output of TWSOA, and (e) Optical spectra at the output of VOA 4 via 'with 3 R regeneration path'

signal's wavelength has changed from 1545 to 1554 nm. The optical spectra at EDFA 3's output is shown in Fig. 2(b). Considering power in the HNLF medium decreases after XPM, VOA 2 is included to compensate for variations in signal power levels and maintain consistency as well as reliability in the communication system. Moreover, EDFA 2 is employed to strengthen the signal resulting from VOA 2. Optical Filter 2 separates the signals at 1545 nm and 1554 nm and lessens undesired sidebands. Fork splits obtained signal into two paths—one with 3R regeneration andthe other without—for additional processing.

The converted signal at 1554 nm has a received power of 24 dBm, which is 19 dBm more than the power received at HNLF. The noise signal's power is now less than −100 dBm, indicating significantly better signal quality.

The optical spectra at VOA 3 in the 'without 3R regeneration path' is shown in Fig. 2(c). With a received power of −27 dBm, the original probe signal is totally shifted at wavelength 1554 nm, and the signal at 1545 nm is eliminated. It demonstrates that there are no sidebands at 1554 nm. The noise level is less than −100 dBm and the received power is saturated. Fig. 2(d) displays the power spectrum at TWSOA as a function of wavelength. This occurs subsequent to the connection of the clock signal with the signal acquired from EDFA 3. The signal is re-timed using the clock signal. At 1554 nm, 24 dBm of power is received. Fig. 2(e) displays the optical spectra at VOA 4 in the 'with 3R regeneration path'. The desired signal at 1554 nm, which contains all of the information of the actual sent signal, is isolated using Optical Filter 3. The Optical Filter 3 attenuates all undesired sidebands. Even after accounting for the noise in TWSOA, OSA indicates that the power received at VOA 4 is −23 dBm, which is 4 dBm more than the power received at VOA 3. Additionally, it is found that −100 dBm is the saturated noise level. The 3R process is carried out by combining the capabilities of TWSOA, Clock, and EDFA 3.

By reducing excessive distortions, the desired wavelength shift is obtained. EDFAs, VOAs, TWSOA, clock, Gaussian optical band pass filters and low pass filters are used to optimize the signal to noise ratio and spectral width.

An electrical signal is produced from an optical signal using a photodetector PIN. The RF spectrum analyzer plots obtained at LPF 1 and LPF 2, respectively, are shown in Fig. 3(a) and Fig. 3(b). For simulation, a cutoff frequency of 60 GHz is used for the LPF. Signals at low frequencies are allowed under LPF. It is noted that when frequency increases, SNR decreases. The RF spectrum analyzer at LPF 1 displays a signal power of −83 dBm without the use of a 3R regenerator, as illustrated in Fig. 3(a).

Additionally, utilizing 3R regeneration at LPF 2, the RF spectrum analyzer displays the signal power at −73 dBm in Fig. 3(b). This indicates that the use of 3R regeneration increases signal power by 10 dBm when compared to not using 3R regeneration.

Using BER analyzers 1 and 2, respectively, Fig. 4(a) and Fig. 4(b) depict the eye diagram of the wavelength-converted signal with and without 3 R regeneration. Green represents the noise power and blue represents the signal power. The strong signal to noise ratio in both eye diagrams demonstrates that the recommended configuration yields a high-quality signal. Two waveforms with a large central area (eye opening) are displayed in both eye diagrams; each corresponds to a distinct bit period. A wide eye opening suggests that a high-quality signal has been received. There are extremely few jitters, indicating a significant decrease in timing errors. The eye diagram amplitude is 550 μ greater with 3R regeneration than it is without it. It may be established that 3R regeneration further boosts

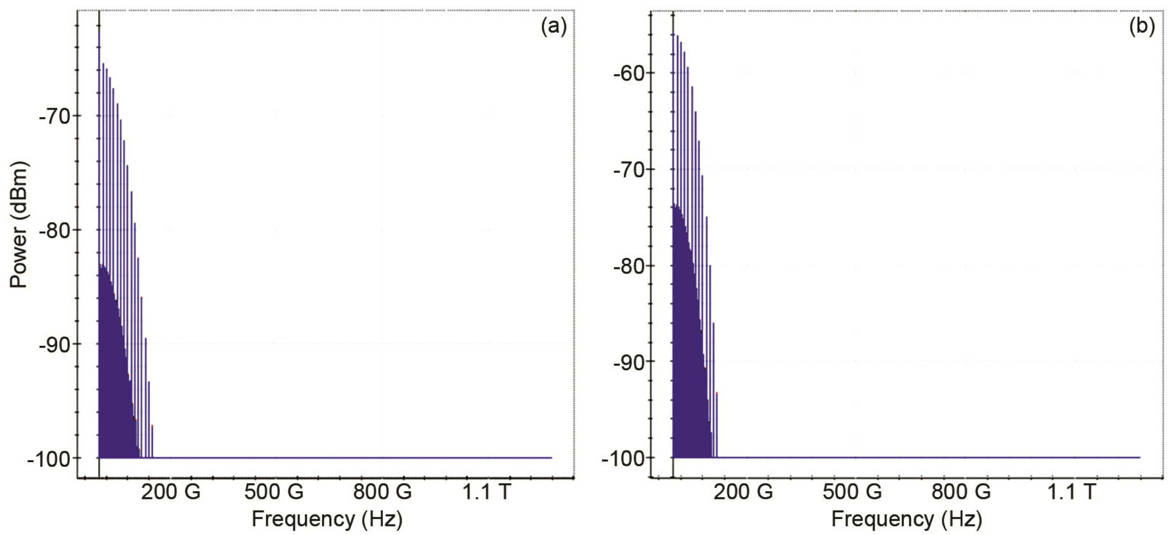

Fig. 3 — (a) RF spectrum analyzer plot at LPF 1, at cut-off frequency 60 GHz and (b) RF spectrum analyzer plot at LPF 2, at cut-off frequency 60 GHz

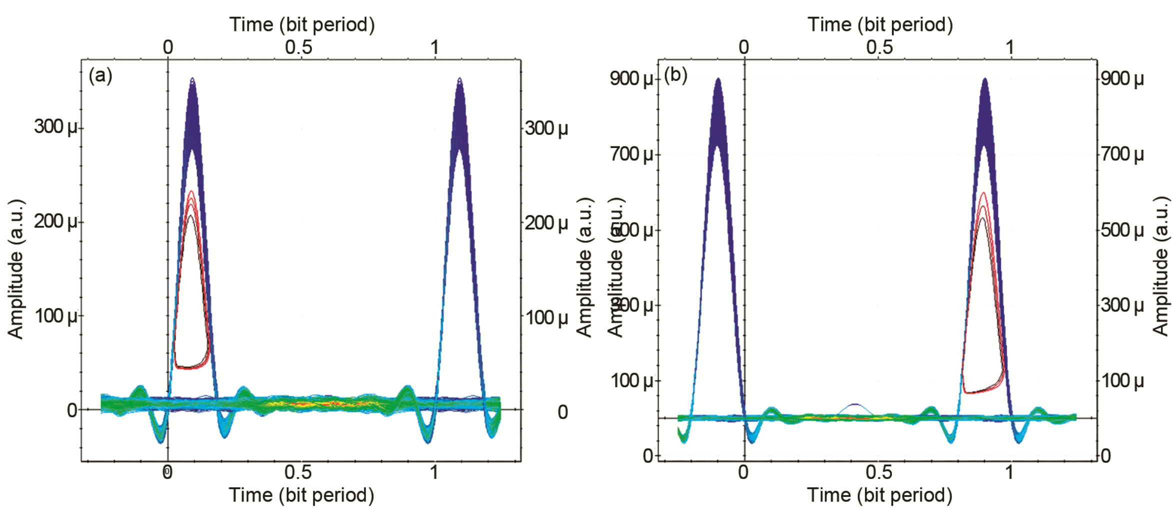

Fig. 4 — (a) Eye diagram of wavelength converted signal without using 3R regeneration, and (b) Eye diagram of wavelength converted signal with using 3R regeneration

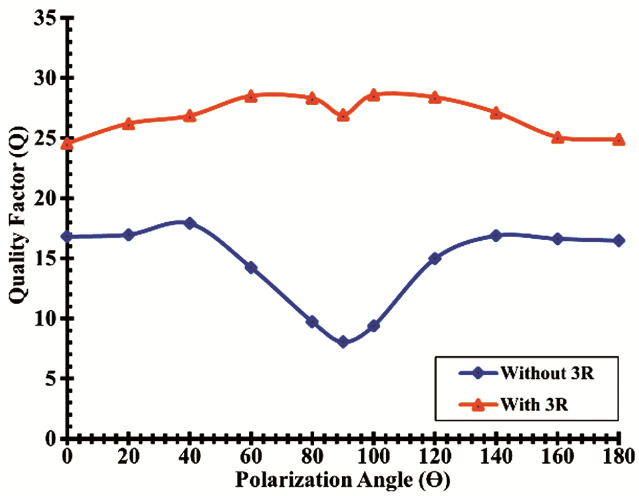

Fig. 5 — Q factor as a function of polarization angle

the SNR because the green edge is thicker and blurred when it is not employed.

The quality factor Q curves in relation to the polarization angle (θ) are shown in Fig. 5. The polarization angle has a 20-degree step size and a range of 0 to 180 degrees. Without 3R regeneration, the maximum Q is 17.89 between 0 and 90 degrees, and 16.88 between 90 and 180 degrees. If 3R regeneration is not used, Q values first follow a decreasing pattern between 0 and 90 degrees, and then an increasing pattern between 90 and 180 degrees. The greatest Q with 3R regeneration is 28.51 between 0 and 90 degrees, and 28.59 between 90 and 180 degrees. When using 3R regeneration, Q values exhibit an increasing pattern between 0 and 90 degrees, followed by a decreasing pattern between 90 and 180 degrees. From both cases, it is evident that the inclusion of 3R regeneration improves the quality factor by more than 19 at a 90-degree angle, and Q curves follow symmetry with respect to orthogonal polarization.

Furthermore, for both the scenario with and without 3R regeneration, the BER curves exhibit their logarithmic values in relation to rotational angle (θ) in Fig. 6. With a 20-degree step size, the rotating angle spans from 0 to 180 degrees. Without 3R regeneration, the minimum logarithmic value of BER is −71.20 between 0 and 90 degrees, and 63.55 between 90 and 180 degrees. If 3R regeneration is not used, BER values first follow an increasing pattern between 0 and 90 degrees, and then a decreasing pattern between 90 and 180 degrees. The lowest logarithmic value of BER with 3R regeneration is −178.42 between 0 and 90 degrees, and −179.35 between 90 and 180 degrees. When using 3R regeneration, BER values exhibit a decreasing pattern between 0 and 90 degrees, followed by an increasing pattern between 90 and 180 degrees. The introduction of 3R regeneration clearly lowers the BER log value from −15.35 to −159.26 at a 90-degree angle in both cases, and the BER curves exhibit orthogonal polarization symmetry. Moreover, Table 1 shows the comparative results with/without 3R regeneration obtained using BER analyzer.

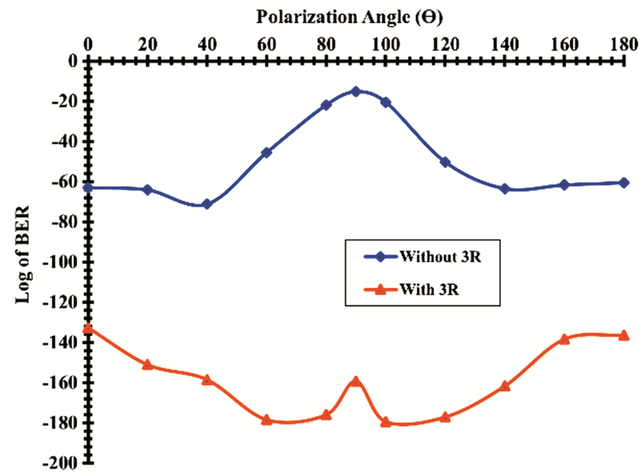

Fig. 6 — BER curves as a function of polarization angle

Table 1 — Results of BER Analyzer

Parameters	Numerical value	
	Without 3R	With 3R
Algorithm	Gaussian	Gaussian
Extinction ratio at min BER (dB) at 180 degrees	15.28	27.89
Max. eye opening factor	0.9396	0.9587
Max. eye opening factor (dB)	−0.27	−0.18
Penalty (dB)	0.27	0.18

Conclusions

The impact of RoPP on XPM-based wavelength conversion using polarization rotator and HNLF is examined in this research. By calculating the Q value and BER for various rotation angles, signal quality is determined. In order to achieve effective wavelength conversion, probe pump interaction on nonlinear media and filter function are tuned. The major finding of this study shows that the symmetry with regard to the orthogonal polarization angle is depicted by the evaluation of BER and Q value as functions of different polarization angles, θ. As a result of 3 R integration, at 90 degrees, the Q value increases to 26.92 from 8.04 and the log of BER decreases to −159.26 from −15.35. By enhancing the functionality of both 3R regeneration and the polarization rotator combined, efficient wavelength conversion can further improve the performance and spectral efficiency of the DWDM optical network.

References

1 Hecht J, *Instructor's Manual to Accompany Understanding Fiber Optics*, (Laser Light Press), (2022) https://doi.org/10.1117/3.2656165.ch12.

2 Modak N, Das S, Bordoloi P & Ghosh N, Interferometric weak value of polarization observable and differential Jones matrix algebra, *J Opt*, **24(3)** (2022) 034009, https://doi.org/10.1088/2040-8986/ac4d72.

3 Agrawal G P, *Applications of Nonlinear Fiber Optics*, (San Diego: Academic Press), (2020).

4 Bhatia R, Sharma A K & Saxena J, Comparative investigations of DWDM transmission system with PMD for different orthogonally modulated signals at 80 Gb/s, *Int J Commun*, **29(6)** (2015) 1084–1090, doi: 10.1002/dac.3076.

5 Singh S, Singh S, Ngo Q M & Mohammadi A M, 340-Gb/s PolSK-DP-DQPSK optical orthogonal modulation format with coherent direct detection for high capacity WDM optical network, *Opt Fiber Technol*, **52** (2019) 101936, https://doi.org/10.1016/j.yofte.2019.101936.

6 Fordell T, Open-loop polarization mode dispersion mitigation for fibre-optic time and frequency transfer, *Opt Express*, **30(4)** (2022) 6311–6319, https://doi.org/10.1364/OE.448553.

7 Wang B, A research on all-optical wavelength conversion technology based on SOA, 11th Int *CPEEE*, (2021), https://doi.org/10.1109/cpeee51686.2021.9383386.

8 Lu J, Meng J, Liu J, Zeng X, Wang Y & Ma J, Polarization insensitive wavelength conversion based on orthogonal pump for polarization multiplexing 16-QAM OFDM signal, *OGC Shenzhen: IEEE*, (2015), https://doi.org/10.1109/OGC.2015.7336856.

9 Sarojini R, Sivanantharaja A & Selvendran S, All-optical wavelength conversion of 80 gbps CSRZ-DPSK data signal using cross polarization modulation in single wideband SOA with sub-mw pump power, *Opt Quant Electron*, **54(314)** (2022), https://doi.org/10.1007/s11082-022-03540-y.

10 Parashuram & Kumar C, Optimal wavelength conversion of 250 Gbps PDM-(DP)QPSK signals based on dual SOA using co-polarized dual pumped FWM, *J Opt*, **53** (2024) 1471–1491, https://doi.org/10.1007/s12596-023-01270-2.

11 Zhao Y, Yan Z, Fu P, Cai Y & Yuan Y, All-optical wavelength conversion based on dual-polarization SOAs for a 112 Gbps PDM-16QAM signal using parallel dual-pump, *OSA Continuum*, **4(4)** (2021) 1125–1134, https://doi.org/10.1364/OSAC.415288.

12 Huo J, Wang J, Wang Y, Shang C, Huangfu W, Liu L, Wang Z, Long K & Wu C, Vector distribution measurement of PMD in optical fiber links employing a wavelength-tunable SOP-OTDR, *Appl Opt*, **61(13)** (2022) 3754–3760, https://doi.org/10.1364/AO.454671.

13 Liu Y, Disentanglement induced by combined effects of polarization mode dispersion and polarization-dependent loss in optical fibers, *Opt Quantum Electron*, **50(720)** (2023), https://doi.org/10.1007/s11082-023-05025-y.

14 Singh K, Kaur G, Bansal M & Gupta V, Performance analysis of a cross-gain modulation (XGM) utilization in bulk-semiconductor optical amplifiers (SOAs) based all-optical 2R regeneration scheme, *J Opt*, (2023) 1–19, https://doi.org/10.1007/s12596-023-01352-1.

15 Li L, Patki P G, Kwon Y B, Stelmakh V, Campbell B D, Annamalai M, Lakoba T I & Vasilyev M, All-optical regenerator of multi-channel signals, *Nat Commun*, **8(884)** (2017), https://doi.org/10.1038/s41467-017-00874-0.

16 Parashuram, Kumar C, InP Photonic Integrated All-Optical Wavelength Conversion of 128 GBaud DP-16QAM Signals using XGM in SOAs, *Wirel Pers Commun*, (2024) 1–20, https://doi.org/10.1007/s11277-024-11121-3.

17 Feng X, Wu Z, Wang X & Gao S, Integrated all-optical wavelength multicasting for 40 Gbit/s PDM-QPSK signals using a single silicon waveguide, *Opt Laser Technol*, **94** (2017) 261–266, https://doi.org/10.1016/j.optlastec.2017.03.039.

18 Shi X, Li Y, Xin N & Wang W, An optical multi-wavelength conversion method for distributed satellite system based on the nonlinearity of SOAs, *ICAITA 2020. Guilin J Phy Conf Ser*, (2020) **1651**, https://doi.org/10.1088/1742-6596/1651/1/012099.

19 Jawad M J & Ghafoor S, All-optical 2R-regeneration and continuous wave to pulsed signal wavelength conversion based on fiber nonlinearity, *Opt Quantum Electron*, **50(366)** (2018), https://doi.org/10.1007/s11082-018-1633-7.

20 Inoue K & Igarashi K, Nonlinear interaction between non-orthogonally polarization-multiplexed signals in fiber transmission with polarization-dependent loss, *Optics Continuum*, **2(10)** (2023) 2225–2234, https://doi.org/10.1364/OPTCON.499394.

21 Maywar D N & Graiti S A A, Demonstration of simultaneous nonlinear polarization rotation and dispersive bistability, *Nonlinear Optics* (*NLO*), (Waikoloa Beach: Optica Publishing Group), (2019), https://doi.org/10.1364/NLO.2019.NM2B.6.

22 Li C, Wei X, Tan S, Kang N C J & Wong K K Y, Short wavelength mode-locked thulium-doped fiber laser based on nonlinear polarization rotation, (CLEO, San Jose: Optica Publishing Group), (2017), https://doi.org/10.1364/CLEO_SI.2017.STu1K.5.

23 Parashuram & Kumar C, Manifestation of varying polarization state of alternating channels in multicasting WDM network and mitigating the impairments using nonlinear OPC and dispersion compensation, *J Opt*, (2024) 1–14. https://doi.org/10.1007/s12596-023-01638-4.

24 Sobhanan A, Anthur A, O'Duill S, Pelusi M, Namiki S, Barry L, Venkitesh D & Agrawal G P, Semiconductor optical amplifiers: Recent advances and applications, *Adv Opt Photonics*, **14(3)** (2022) 571–651, https://doi.org/10.1364/AOP.451872.

25 Leuthold J, Signal regeneration and all-optical wavelength conversion, *The 15th Ann Meet IEEE Lasers and Electro-Optics Society. Glasgow: IEEE*, (2002), https://doi.org/10.1109/LEOS.2002.1133941.

26 Li Q, Wang Z, Wang H, Cui C & Wu C, Artificial neuron based on nonlinear polarization rotation in a semiconductor optical amplifier, *Opt Commun*, **435** (2019) 405–408, https://doi.org/10.1016/j.optcom.2018.11.074.

27 Li W, All-optical generation of frequency-shift keying radiofrequency signal based on nonlinear

polarization rotation in a highly nonlinear fiber, *Nonlinear Optics*, (Kauai: OpticaPublishing Group), (2015), https://doi.org/10.1364/NLO.2015.NTu2A.4.

28 Zali A R, Stabile R & Calabretta N, Polarization insensitive photonic integrated 1x4 WDM wavelength selective switch for optical networks, *Opt Fiber Commun Conf*, (San Diego: Optica Publishing Group), (2023), https://doi.org/10.1364/OFC.2023.Tu2E.2.

29 Sakaguchi J, Nishida T & Ueno Y, 200-Gb/s wavelength conversion using a delayed-interference all-optical semiconductor gate assisted by nonlinear polarization rotation, *Opt Commun*, **282(9)** (2009) 1728–1733, https://doi.org/10.1016/j.optcom.2009.01.028.

30 Singh S, Ye X & Kaler R S, All optical wavelength conversion based on cross polarization modulation in semiconductor optical amplifier, *J Light Technol*, **31(11)** (2013) 1783–1792, https://doi.org/10.1109/JLT.2013.2252326.

31 Huo L, Zhang E & Lou C, Clock Recovery for OTDM and 3R Regeneration, in *Info Optoelectron Nanofab Test*, (Wuhan: Optica Publishing Group), (2012), https://doi.org/10.1364/IONT.2012.IF1B.2.

32 Sarojini R, Sivanantha A R, Selvendran S & Esakki K M, Cross polarization modulation based wavelength conversion with very low pump power in SOA: An investigation, *Optik*, **185** (2019) 852–858, https://doi.org/10.1016/j.ijleo.2019.04.016.

33 Singh S & Singh S, Design of optical wavelength conversion based on cross polarization modulation effect of SOA-MZI, *Opt Quantum Electron*, **52(122)** (2020).